# Motion and Grasping Control Method of 2-DOF Robotic Finger

Mariam Md Ghazaly[1,2]*, Mohamad Adzeem Mohamad Yuden[1,2], Aliza Che Amran[1,3]
[1]Center for Robotic and Industrial Automation (CeRIA), Universiti Teknikal Malaysia Melaka, Hang Tuah Jaya, 76100 Durian Tunggal, Melaka, Malaysia
[2]Fakulti Kejuruteraan Elektrik, Universiti Teknikal Malaysia Melaka, Hang Tuah Jaya, 76100 Durian Tunggal, Melaka, Malaysia
[3]Fakulti Kejuruteraan Teknologi Elektrik dan Elektronik, Universiti Teknikal Malaysia Melaka, Hang Tuah Jaya, 76100 Durian Tunggal, Melaka, Malaysia
*Corresponding Email: mariam@utem.edu.my

***Abstract*— The focus of this paper is the grasping control and tracking performances for the two degrees of freedom (2-DOF) robotic finger mechanism in accomplishing precision motion control as the initial study in the development of a multi-fingered robotic hand system. In the robotic hand mechanism, behaviours like large steady-state error, instability, and poor transient performance are often observed. For this research, the proposed controllers will rely on each motor joint's angular position control, which refers to the position control possessed by the 2-DOF robotic finger mechanism. Three various control approaches namely (i) Fuzzy Logic controller (FLC) (ii) Proportional Integral Derivative (PID) controller and (iii) Linear Quadratic Regulator (LQR) controllers were selected for comparison via experimental and simulation works. Validation of the controller results was performed by tracking control and grasping control, with frequency ranges from 0.1 Hz to 0.5 Hz at various reference amplitudes. Based on the results of the analysis, it was concluded that LQR controller had the best performance for tracking control. The LQR controller exhibited a 98.5% (0.11 °) improvement in steady-state error compared to an uncompensated system based on a series of experimental tracking tests. Another conclusion was that the 2-DOF robotic finger mechanism was also successful in grasping tasks with the Fuzzy controller being used by the specific reference trajectory.**

***Index Term*— motion tracking, grasping, controller, robotic finger**

## I. Introduction

Nowadays, the industry sector is widely utilising robotic hands. In recent years, there has been a drastic increase in the demands for robotic hands system with high precision performance. Generally, the robotic hands have a vital part in achieving higher accuracy, larger productivity, and increased flexibility, particularly in the manufacturing process. Recently, numerous researchers have built robotic hands that have their own novel mechanisms and designs. However, compared to human hands, existing robotic hands are quite heavy because of the weight of the actuators and the complex transmission mechanisms [1], [2]. The challenges in designing the robotic hands are due to the complex mechanical structure that is needed to control a vast amount of DOFs and actuators, which lead to very complex systems at high costs [3-5]. Apart from this, the utilisation of high precision performance of robotic hand system has experienced a radical growth in recent years, particularly in the industrial sector. Some of the issues in controlling robotic finger mechanism include the control inputs itself and the external disturbances that give rise to positioning errors and flexural vibrations on the structures of the robotic finger mechanism [6-8]. In the industrial field, robotic hands require higher performance for them to do precise and dexterous works. However, current robotic are faced with the problem of having low precision positioning performances, robbing them of the capacity to be used for precision and dexterous tasks. For instance, robotic hands still have some limitations in the robotic assembly cell for precise and small production.

Robotic hands have limited dexterity for grasping small objects because of their low precision motion. Based on previous studies [9], robotic hands have been successful in performing power grasps but have issues with performing precision and dexterous tasks on significantly smaller objects. For majority of prosthetic hands, the combination of position and force control is utilised for non-contact and contact tasks, respectively. This technique does not have a proper transition between the various steps. Furthermore, it needs to precisely measure contact position in order to achieve a stable grasp [10]. Furthermore, some robotic hands may not work well in real time because assessing the target joint angle from the fingertip position may take a longer time [11]. Conventionally controlling these robotic hands for one DOF may also need too much concentration from one input. There is a need to use novel design methodologies to address the issue of low functionality of robotic hands while simultaneously satisfying their mass and size requirements [12, 13]. Control and stability are needed to construct a robotic hand that has the ability to perform just as well as a human's. Robotic hands therefore need precise motion control that allows them to follow the exact trajectory in order to meet an expected outcome. Therefore, it is desirable to have a high motion control controller design for improving the precision motion performance of the robotic hand system.

## II. Robotic Hand Prototype

### A. Experimental Setup

In this study, the developed robotic hand is made up of four active fingers. This was done in order to reduce costs and ensure enough flexibility for the purpose of the operation. Every finger is equipped with two links and 2-DOF. On the other hand, the thumb possesses three links and 3-DOF to allow abduction and adduction movements. Thus, the developed robotic hand can be classified as having 9-DOF. In this study, the 2-DOF fingers and two links that were utilised

were made up of a proximal pin joint and a distal flexure joint. For these fingers, the basic design is determined by the needs of a general purpose hand. Changes like the utilisation of a bevel gear at the proximal joint and the lengthening of the distal link were chosen to enhance the capacity of the robotic hand to exert larger fingertip forces for object manipulation. Since the finger is made up of 2-DOF, motion uncertainty has two actuators. Therefore, the fingertip has a slightly curved design to lessen the extra DOFs. As a result, there is an extension of the finger motion to three dimensional spaces. Furthermore, it will only need two DC micro motors for driving the finger. In this study, the designed robotic hand is 257 mm long, 100 mm wide, and 20 mm thick when it is fully spread. This robotic hand's total mass is approximately 444 g, which includes the circuit boards.

The design and selection of the appropriate palm size is vital in preventing limited or reachable working range. Generally, the robotic hand's function depends on the performance of the actuator. For this study, each finger joint is actuated using a Faulhaber DC micro motor. This motor is used because it is more stable in terms of response time, reliability, and efficiency. For this robotic hand, the actuation mechanism is made up of a DC micro motor, bevel gear, a planetary gearhead, and an optical encoder. In the beginning, a tendon drive mechanism was considered for actuating the finger, but was later abandoned due to its small grasping focus. Therefore, a collection of bevel gears is responsible for transmitting the torque between joints. The utilisation of bevel gear offers more precise knowledge of joint position to lessen the effect of elasticity and hysteresis of the transmission system. Moreover, there should be careful selection of the amount of teeth of the bevel gear in order to generate the desired output torque. The variations in the amount of teeth could result in varying diameters, which influence the entire mechanism design. Bearings are required for correctly placing the shaft. If the shaft is in the right position, one can achieve an accurate angle during the opening and closing the finger's holder. The setting of the developed robotic hand is depicted in Figure 1 and Figure 2, respectively.

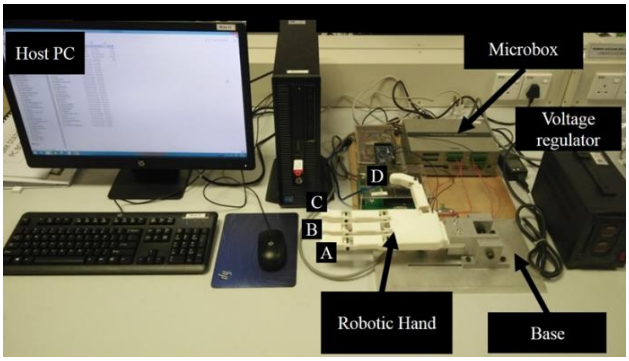


Fig. 1. Experimental setup for the developed robotic hand

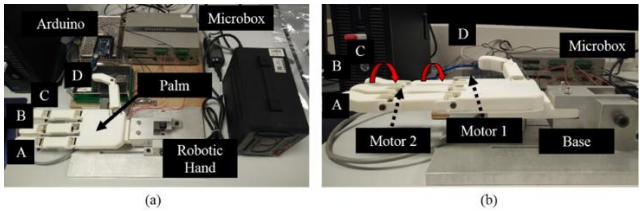


Fig. 2. View of the developed robotic hand (a) isometric view, (b) side view

### B. 2-DOF Robotic Finger Mechanism

In this research, there will be an evaluation of the 2-DOF robotic finger mechanism labelled as 'B' and illustrated in Figure 3. This paper only examines one finger to serve as an initial study towards the construction of a multi-fingered robotic hand. The mechanism of the 2-DOF robotic finger is made up of two joints and two links, where every actuator in the joint is fitted within the palm and robotic finger link. The 2-DOF robotic finger possesses two links, L1 and L2, which rotate because of the DC micro motor located at joints P and Q, respectively. L0 represents the displacement between the joint P and the robotic hand palm. Figure 3 shows the schematic design of the 2-DOF robotic finger that was formulated in this research. Each joint of the robotic finger is attached using shaft so that it can deliver motion for every link and smoothly move the 2-DOF robotic finger like a human hand. For this study, the end of the distal segment of fingertip is slightly curved to assist with object manipulation. By utilising the proposed mechanism, it was able to construct a multi-jointed robot finger. This 2-DOF robotic finger is advantageous because it is lightweight and compact. Table I illustrates in detail parameter design of single 2-DOF robotic finger mechanism.

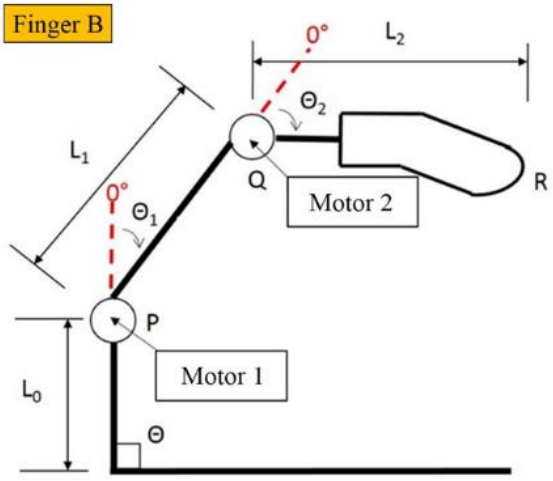


Fig. 3. Schematic diagram of 2-DOF robotic finger (Finger B)

TABLE I
PARAMETER SPECIFICATIONS OF 2-DOF ROBOTIC FINGER

| Parameters | Value |
|---|---|
| Dimension (L x W) | 133 mm x 25 mm |
| Mass | 57.8 g |
| Number of link | 2 |
| Degrees of freedom | 2-DOF x 1 finger |
| Articulation sensor | Optical encoder |
| Actuator | Faulhaber DC micro motor |
| Link rotation limitation | Link 1; 0°<Θ<90°<br>Link 2; 0°<Θ<90° |

In this research work, during the positioning experiment, measurement of the angular positions for links 1 and 2 is done. The joint angle for links 1 and 2 defines the desired position regarding the 2-DOF robotic finger. As shown in Figure 3, theta represents the joint angle with regards to finger link axis and robotic hand palm axis. For each robotic finger, the joint angular position, theta, lies between 0° (minimum) and 90° (maximum). Actually, for both links 1 and 2, the mechanism is comparable, while mass being the only difference between both. The 2-DOF robotic finger mechanism pertaining to link 2 is positioned on top of link 1, thus the weight of the link 2

has to be endured by link 1. The 2-DOF robotic finger mechanism for Link 1 makes the load 1.5 times heavier when compared with the link 2 since link 2 is positioned on top of link 1.

## III. Motion and Grasping Control – Design Procedure

### A. Proportional Integral Derivative (PID) Controller

The PID control method has been built to improve the system performance pertaining to the 2-DOF robotic finger, including steady-state error, percentage of overshoot and response time. After applying the PID controller, a comparison of the results is done with the uncompensated closed-loop system. Matlab Simulink application is employed for running the control program. Better output results are achieved by tuning PID parameters with regards to overshoot, response time and error for the joint motor control. In this research work, the design of the PID controller allows swift responses of output parameter and keeps the error to minimum during position control. A block diagram structure showcasing the mechanism of 2-DOF robotic finger for PID position control employed in this study is presented in Figure 4.

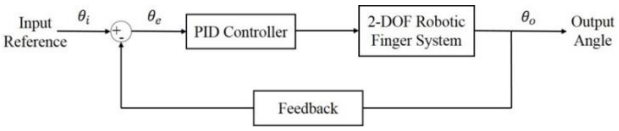


Fig. 4. Block diagram structure of the compensated closed-loop system with PID controller

In this study, the Ziegler-Nichols closed-loop tuning method is employed to design the PID controller representing the system to determine the PID control parameters pertaining to the motor's joint for the 2-DOF robotic finger. In this paper, $K_u$ represents the obtained ultimate gain value, i.e. 54.6, and $P_u$ signifies the period of oscillation, i.e. 0.015. Into the Ziegler-Nichols closed-loop equations, these values are replaced to get the approximated parameters. Table II presents the Ziegler-Nichols tuning formula method that has been employed in this research study. Equation (1) shows the PID controller consisting of integral, proportional and derivative components as well as the general equation pertaining to PI, P and PID controller.

$$G_{PID} = K_p + \frac{K_i}{s} + K_d s \quad (1)$$

TABLE II

ZIEGLER-NICHOLS TUNING FORMULA METHOD

| Control Type | $K_p$ | $K_i$ | $K_d$ |
|---|---|---|---|
| P | $0.50 \times K_u$ | - | - |
| PI | $0.45 \times K_u$ | $0.85 \times P_u$ | - |
| PID | $0.60 \times K_u$ | $0.50 \times P_u$ | $0.13 \times P_u$ |

### B. Fuzzy Logic Controller (FLC)

The control method FLC follows a linguistic approach, which is derived from expert knowledge regarding an automatic control method. The linguistic rules define FLC's control actions. A form of quantification pertaining to imprecise information (input Fuzzy sets) is applied through generation of an inference scheme, which is derived from a knowledge base of control position that can be applied to the system. Figure 5 presents a block diagram structure pertaining to the compensated closed-loop system along with FLC.

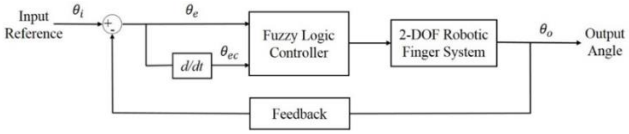


Fig. 5. Block diagram structure of the compensated closed-loop system with FLC

In this paper, application of centroid defuzzification technique and Mamdani-type inference technique to the system is done. A two input and one output system is applied for the compensated closed-loop system with FLC. The system inputs include rate of change of error (*ce*) and steady-state error (*e*); meanwhile, the angle of the 2-DOF robotic finger mechanism is the output. An error can be described as reference angle that is subtracted by output angle, in which the rate of error change is defined as the current values that is subtracted by the previous values of error. The Gaussian Fuzzifier was employed for the input, and the triangular for the output. In this research work, the Fuzzy error set is fixed to −5 to 5 degrees, the derivative error ranging from −500 to 500 degrees, and the motor output is set from −50 to 50 degrees, which equals the position that can be applied to each joint to get the desired angle. Figure 6 presents the membership functions pertaining to the two inputs and one output variables of FLC employed in this research work.

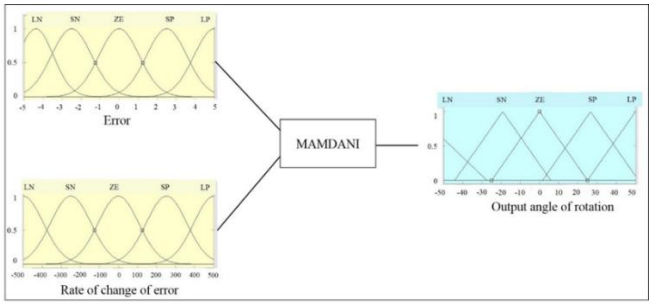


Fig. 6. All membership functions for two inputs and one output variables of FLC

### C. Linear Quadratic Regulator (LQR) Controller

LQR controller is according to the state space system and the Algebraic Riccati equation is solved to obtain the optimal control input. Figure 7 shows the LQR control system used in this study.

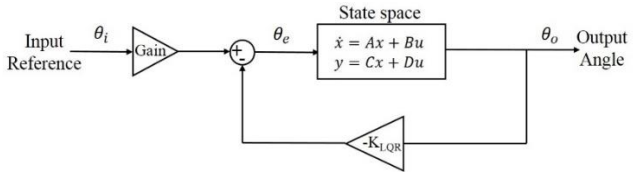


Fig. 7. Block diagram structure of the compensated closed-loop system with LQR controller

A linear time-invariant system is taken into account as depicted in Equation (2).

$$\dot{x}(t) = Ax(t) + Bu(t) \quad (2)$$

where, $\dot{x}$ is the state variable and u is the control input variables.

The design of LQR controller is aimed at determining $K_{LQR}$, which is the state-feedback control vector, to get $u(t)$, i.e. the control vector. Equation (3) expresses the linear state feedback control law, which is determined by the minimisation of a quadratic cost function as presented in Equation (4). Then, the Riccati solution, $P$, expressed in Equation (5), is produced by the Algebraic Riccati Equation. The first aim here is to determine the state feedback control law pertaining to the designing process in a bid to keep the cost function index to minimal.

$$u(t) = -K_{LQR}x(t) = -R^{-1}B^{T}Px(t) \quad (3)$$

$$J = \int_{0}^{\infty}[x^{T}(t)Qx(t) + u^{T}(t)Ru(t)]dt \quad (4)$$

$$A^{T}P + AP - PBR^{-1}B^{T}P + Q = 0 \quad (5)$$

Here, $Q$ represents the diagonal weight matrix, i.e. positive definite $(Q > 0)$, and $R$ signifies the weight factor, i.e. positive semi-definite $R \geq 0$. The design of the LQR controller is built upon the minimisation of quadratic performance index, $J$, and the values for $Q$ and $R$ are chosen based on appropriate weightings for the system state. For the system, the optimum $Q$ matrix was found to be [8 0, 0 8]. The $Q$ matrix's gains summation was 9.0 V, which denotes the upper limit pertaining to the digital signal processing unit. Consequently, Matlab was employed to transform $R$ weight factor and design $Q$ diagonal weight to produce the state-feedback control gains, $K_{LQR}$. The Matlab commands are shown in Equation (6).

$$K = lqr(A, B, Q, R) \quad (6)$$

In this study, the optimum diagonal of the $Q$ matrix was found to be equal to [8 0, 0 8], in which the value of $R$ was equal to 1. Based on these designed weight parameters, the state-feedback control gains, $K_{LQR}$, were found to be $[0.9233 \quad 1.7346]$ concerning Motor 1 and $[2.0927 \quad 208299]$ concerning Motor 2.

## IV. Results And Discussions

### A. Tracking Control Experiment

For difference reference angles, wave tracking control experiments were performed for the compensated closed-loop sinusoidal. The tracking experiments' aim was to demonstrate that the put forward control methods can follow commanded trajectories to induce a 2-DOF robotic finger movement. To see the impacts of various frequencies on the output signals, the system's frequency was varied. For tracking motion, sinusoidal reference inputs containing three different frequencies (0.1 Hz, 0.2 Hz and 0.5 Hz) and three different amplitudes (15°, 30° and 40°) were evaluated. Each of the experiment set was carried out 10 times to see how the said controllers would adapt in tracking motion. The system's frequency is modified to observe the impacts of various frequencies on the output signals. The evaluation of the position tracking controller pertaining to the 2-DOF robotic finger's joint was done alongside a sinusoidal reference signal. For the experiments, the sampling time was set at 0.001 sec. Table III lists out the parameters that were fixed and modified for the control experiments of compensated closed-loop sinusoidal wave tracking.

TABLE III
PARAMETERS FOR SINUSOIDAL WAVE TRACKING ERROR EXPERIMENTS

| Parameter | Numerical Value |
|---|---|
| Reference type | Sinusoidal wave |
| Reference angle | 15 °, 30 °, 40 ° |
| Frequency | 0.1 Hz, 0.2 Hz, 0.5 Hz |
| Simulation time | 6 s |
| Starting time | 0.5 s |
| Sampling time | 0.01 |

### B. Grasping Control Experiment

The proposed controllers' practicality was evaluated through grasping tracking experiment that analysed the tracking control's performance via a single 2-DOF robotic finger mechanism. The robustness of the designed FLC, PID and LQR controller was determined by employing the continuous stepwise wave signal. The purpose of this grasping tracking was to confirm the put forward control methods' ability to follow a desired trajectory. Identification is done for a set of position data to get the grasping trajectory pertaining to 2-DOF robotic finger joints for the position reference design.

Various aspects need to be kept in mind when designing the reference trajectory for grasping motion, like the types of objects, weight of the object, object surface and optimal grasping style. In this paper, the desired grasping style is generated by determining the correct angles for the 2-DOF robotic finger joints. In this case, the trajectory pertaining to grasping of solid objects is generated with the reference position design for 2-DOF robotic finger joints. It was settled that the best angle to grasp the object for Motor 1 is 25° and 40°, and for Motor 2, it is 30° and 40°. The setting of 2-DOF robotic finger's initial joint position for grasping tracking was done at 0°. After this, the 2-DOF robotic finger was set so that it can rotate not only for the flexion/extension but also rotate back for finger links' abduction/adduction. Table IV presents the parameters that were fixed and changed in the compensated closed-loop grasping tracking control experiments.

TABLE IV
PARAMETERS FOR GRASPING TRACKING EXPERIMENTS

| Parameter | Numerical Value |
|---|---|
| Reference type | Grasping trajectory |
| Joint angle | Joint 1: 25 ° and 40 °<br>Joint 2: 30 ° and 40 ° |
| Frequency | 0.1 Hz, 0.2 Hz, 0.5 Hz |
| Simulation time | 6.0 s |
| Starting time | 1.0 s |
| Sampling time | 0.001 s |

### C. Tracking Control Performances

The analysis was conducted based on the frequency and variation angle in sinusoidal input reference pertaining to the

compensated closed-loop tracking control. Figures 8 to 11 showcase the experimental sinusoidal tracking responses pertaining to the FLC, PID and LQR controlled system. For each of the experiment set, Tables V and VI list out the tabulation for the maximum error.

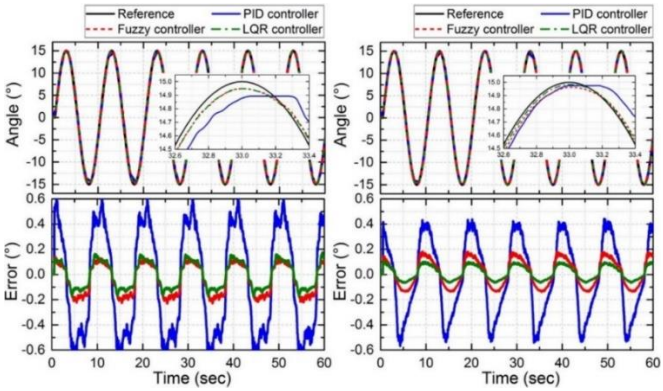


(a) (b)

Fig. 8. Compensated closed-loop sinusoidal tracking response at frequency of 0.1 Hz with reference angle 15 ° (a) Motor 1 and (b) Motor 2

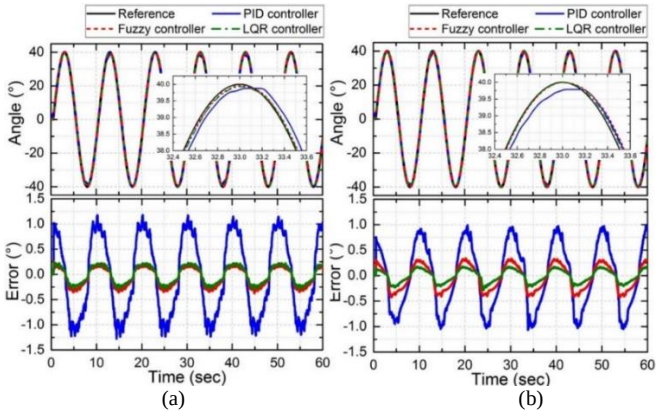


(a) (b)

Fig. 9. Compensated closed-loop sinusoidal tracking response at frequency of 0.1 Hz with reference angle 40 ° (a) Motor 1 and (b) Motor 2

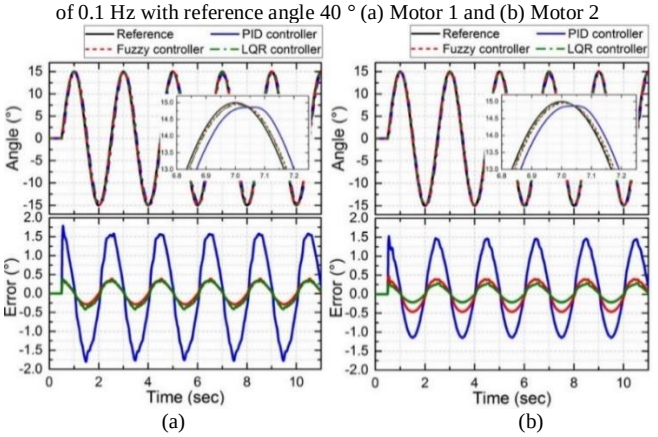


(a) (b)

Fig. 10. Compensated closed-loop sinusoidal tracking response at frequency of 0.5 Hz with reference angle 15 ° (a) Motor 1 and (b) Motor 2

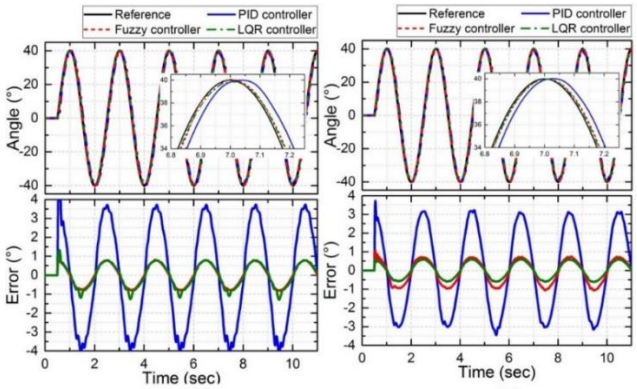


(a) (b)

Fig. 11. Compensated closed-loop sinusoidal tracking response at frequency of 0.5 Hz with reference angle 40 ° (a) Motor 1 and (b) Motor 2

TABLE V

MAXIMUM ERROR FOR TRACKING TESTS OF MOTOR 1

| Controller | | PID | FLC | LQR |
|---|---|---|---|---|
| Frequency (Hz) | Reference Angle (°) | Maximum Error (°) | Maximum Error (°) | Maximum Error (°) |
| 0.1 | 15 | 0.64271 | 0.14100 | 0.17503 |
| | 40 | 1.17542 | 0.25037 | 0.22756 |
| 0.5 | 15 | 1.78984 | 0.40276 | 0.38143 |
| | 40 | 6.23171 | 0.81341 | 1.32770 |

TABLE VI

MAXIMUM ERROR FOR TRACKING TESTS OF MOTOR 1

| Controller | | PID | FLC | LQR |
|---|---|---|---|---|
| Frequency (Hz) | Reference Angle (°) | Maximum Error (°) | Maximum Error (°) | Maximum Error (°) |
| 0.1 | 15 | 0.44216 | 0.18152 | 0.10541 |
| | 40 | 0.98796 | 0.33758 | 0.17610 |
| 0.5 | 15 | 1.52462 | 0.47760 | 0.30207 |
| | 40 | 3.72011 | 1.06218 | 0.61006 |

### *D. Grasping Control Performances*

With regards to the grasping solid object, the best angle for grasping the object for Motor 1 was settled at 25° and 40°, while for Motor 2, it was 30° and 40°. Figure 12 presents the experimental behaviour pertaining to the 2-DOF robotic finger that was managed with continuous FLC, PID and LQR controller. Based on the obtained results, the experimental grasping tracking control was provided for the 2-DOF robotic finger that had the capability to achieve the desired reference signal. It was seen that the proposed reference position pertaining to the desired configuration could be followed by the motor joints.

As seen from the results, the improvements achieved in the response time and steady-state error with the FLC, PID and LQR controller were comparable to that of the uncompensated closed-loop system. Successful achievement of the FLC, PID and LQR control scheme as well as the suggested reference position was recognised, in which the performance of FLC was found to be better versus PID and LQR controller with regards to accuracy and overshooting of the grasping motion.

Through FLC control scheme for the object manipulation, it was found that the proposed reference position was followed by the motor joints of the 2-DOF robotic finger precisely. A good performance was demonstrated by the grasping tracking signal of PID control, in which an error of just 0.05° was seen.

The FLC showed the ability of the controller for good performance with regards to the controller robustness pertaining to the designed grasping tracking signal. The integration of the FLC control enabled stability for the object and the ability of micro gripper to hold the object correctly as well as confer stability during 2-DOF robotic finger operation. As presented in Figure 13, based on the experimental results, the reference trajectory and the FLC control could be applied successfully to enable real-time grasping for solid objects. The experimental results confirmed the successful working of the designed reference position to offer grasping styles as well as sufficient managing of the 2-DOF robotic fingers by the FLC control to achieve the desired task in real time. It can be seen that the suggested reference position of the desired configuration was followed by the motor joints and could also grasp the object efficiently.

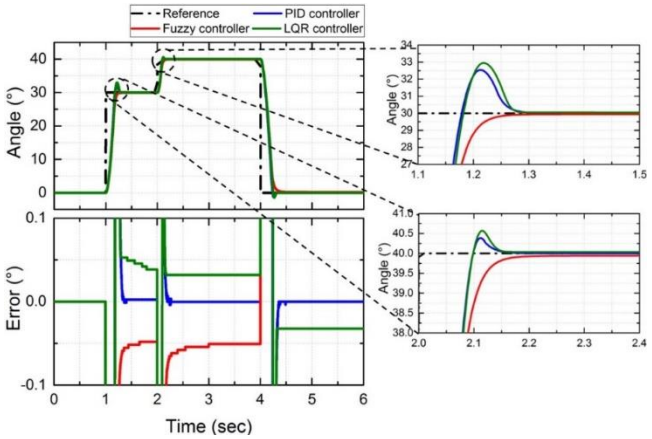


Fig. 12. Experimental compensated closed-loop grasping tracking response

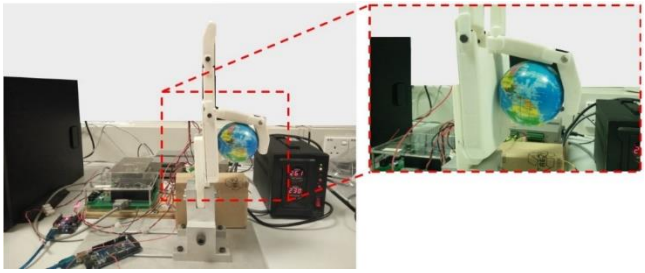

Fig. 13. Grasping solid object experiment of 2-DOF robotic finger

## V. Conclusions

Based on the tracking experimental results, one point was clear that all of the three controllers that were put forward produced good results; however, better robust performance was achieved with the LQR control scheme versus PID and FLC with regards to the final point error and tracking error when employing various reference angles. These results showed that better functioning and accuracy were achieved with the LQR control approach exhibit versus FLC and PID. The LQR controller showed enhancements in steady-state error by 98.5% (0.11°) when compared with the uncompensated closed-loop system when a series of experimental tracking tests were carried out. Apart from this, the grasping task was also successfully achieved by the 2-DOF robotic finger mechanism with the recommended position reference trajectory. In this paper, the desired grasping style was achieved by determining the correct angles pertaining to the 2-DOF robotic finger joints. In conclusion, the FLC was helpful in maintaining the 2-DOF robotic finger at PTP motion, while the LQR controller was apt for continuous tracking motion. Hence, for future work as well as to enhance the current research, the put forward control schemes can be easily extended to multi-fingered robotic hand mechanism and can be applied to articulated mechanism as well.

## Acknowledgment

The authors wish to express their gratitude to Motion Control Research Laboratory (MCon Lab), Center for Robotics and Industrial Automation (CeRIA) and Universiti Teknikal Malaysia Melaka (UTeM) for supporting the research and publication. This research is supported by Ministry of Education Malaysia **(**MOE**)** under the Fundamental Research Grant Scheme (FRGS) grant no. FRGS/2018/FKE-CERIA/F00353.

## References

[1] S. Nishino, N. Tsujiuchi, T. Koizumi, H. Komatsubara, T. Kudawara, and M. Shimizu, "Development of robot hand with pneumatic actuator and construct of master-slave system," Annu. Int. Conf. IEEE Eng. Med. Biol. - Proc., vol. 1, pp. 3027–3030, 2007.

[2] T. Nuchkrua, T. Leephakpreeda, and T. Mekarporn, "Development of robot hand with Pneumatic Artificial Muscle for rehabilitation application," Nano/Molecular Med. Eng. (NANOMED), 2013 IEEE 7th Int. Conf., pp. 55–58, 2013.

[3] F. Inel and L. Khochmane, "Comparison performance between PID and PD controllers for three and four cable based Robots", World Journal of Engineering, vol. 11, no. 6, pp. 543-556, 2014.

[4] M.A.M. Yuden, , M.M. Ghazaly, A.C. Amran, I.W. Jamaludin, H.Y. Khoo, M. R. Yaacob, Z. Abdullah, C.K. Yeo, "Positioning Control Performances Of A Robotic Hand System", Jurnal Teknologi, vol. 79, no. 1, pp. 25-33, 2017.

[5] H. Huang, E. Dong, M. Xu, J. Yang, K.H. Low, "Mechanism design and kinematic analysis of a robotic manipulator driven by joints with two degrees of freedom (DOF)", Industrial Robot, vol. 45, no. 1, pp. 34-43, 2018.

[6] M. Khairudin, Z. Mohamed, and A. R. Husain, "Dynamic Model and Robust Control of Flexible Link Robot Manipulator," Telkomnika, vol. 9, no. 2, pp. 279–287, 2011.

[7] A. Polotto, F. Modulo, F. Flumian, Z. G. Xiao, P. Boscariol, and C. Menon, "Index finger rehabilitation/assistive device," in Proceedings of the IEEE RAS and EMBS International Conference on Biomedical Robotics and Biomechatronics, 2012, pp. 1518–1523.

[8] M. Khuzair, "PID Position Control of Three - Fingered Hand for Different Grasping Styles," in 2015 IEEE 6th Control and System Graduate Research Colloquium (ICSGRC), pp. 9–12, 2015.

[9] J. Schuurmans, R. Q. Van Der Linde, D. H. Plettenburg, and F. C. T. Van Der Helm, "Grasp force optimization in the design of an underactuated robotic hand," in 2007 IEEE 10th International Conference on Rehabilitation Robotics, ICORR'07, 2007, pp. 776–782.

[10] J. L. Pons, E. Rocon, R. Ceres, D. Reynaerts, B. Saro, S. Levin, and W. Van Moorleghem, "The MANUS-HAND Dextrous Robotics Upper Limb Prosthesis: Mechanical and Manipulation Aspects," Auton. Robots, vol. 16, no. 2, pp. 143–163, 2004.

[11] X. T. Le, W. G. Kim, B. C. Kim, S. H. Han, J. G. Ann, and Y. H. Ha, "Design of a flexible multifingered robotics hand with 12 D. O. F and its control applications," in 2006 SICE-ICASE International Joint Conference, 2006, pp. 3461–3465.

[12] Z. Kappassov, Y. Khassanov, A. Saudabayev, A. Shintemirov, and H. A. Varol, "Semi-anthropomorphic 3D printed multigrasp hand for industrial and service robots," 2013 IEEE Int. Conf. Mechatronics Autom. IEEE ICMA 2013, pp. 1697–1702, 2013.

[13] S.-Y. Jung, S. Kang, M. Lee, and I. Moon, "Design of Robotic Hand with Tendon-driven Three Fingers," in 2007 International Conference on Control, Automation and Systems, pp. 83–86, 2007.